
CEPC polarization simulations

Zhe Duan

Institute of High Energy Physics, CAS, China

EPOL Workshop 2022

2022. 09. 22

This presentation is based on the work reported in a modified version of the following preprint:
W. H. Xia, Z. Duan, Y. W. Wang, B. Wang, J. Gao, arXiv:2204.12718v1 [physics.acc-ph]
D. P. Barber is a new collaborator in this study.

Overall progress in CEPC polarization studies

- Study of the radiative depolarization effects in CEPC collider rings [1] (this talk)
 - Spin tracking simulations for CEPC CDR lattice
 - Comparison between simulations with theories
- Longitudinally polarized colliding beams (Tao Chen's talk)
 - Polarization maintenance via the “spin resonance free” feature of the CEPC booster lattice [2,3]
 - Spin rotator design at CEPC-Z energy [4]
- Resonant depolarization (Sep 29 WP1 talk)
 - The option to prepare polarized e⁺/e⁻ bunches from the injector
- Compton polarimeter via scattered electron distribution [5]

[1] W. H. Xia, Z. Duan, Y. W. Wang, B. Wang, J. Gao, arXiv:2204.12718v1 [physics.acc-ph]

[2] V. Ranjbar, et al., PRAB 21, 111003 (2018). [3] Z. Duan, presentation at eeFACT 2022.

[4] W. Xia et al., RDTM (2022) doi: 10.1007/s41605-022-00344-2

[5] S. H. Chen et al., JINST 17, P08005, (2022)

Outline

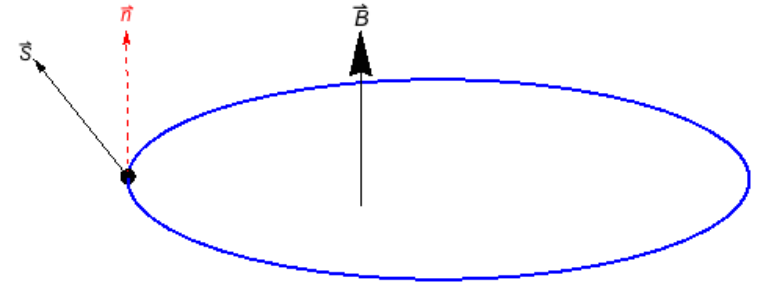
- Radiative depolarization theories
- Simulation setup
- Comparison between the theories and simulations

We'd like to acknowledge kind help from E. Forest (KEK) and D. Sagan (Cornell) regarding usage of BMAD/PTC.

Basics of spin motion in a storage ring

$$\frac{d\vec{S}}{dt} = \vec{\Omega} \times \vec{S},$$

$$\vec{\Omega} = -\frac{e}{m\gamma} \left[(1 + G\gamma)\vec{B}_\perp + (1 + G)\vec{B}_\parallel - \left(G\gamma + \frac{\gamma}{\gamma + 1} \right) \frac{\vec{\beta} \times \vec{E}}{c} \right].$$



- Invariant spin field \hat{n} : $\hat{n}(\vec{z};\theta) = \hat{n}(\vec{z};\theta + 2\pi)$, reduce to \hat{n}_0 on the closed orbit
- Amplitude-dependent spin tune ν_s
 - Reduce to ν_0 on the closed orbit
 - in planar ring: $\nu_0 \approx G\gamma$, $\sim 103.5 @Z$, $181.5 @W$ and $272.5 @H$
- Adiabatic invariant $J_s = \vec{S} \cdot \hat{n}$
- Time-averaged beam polarization $P_{avg} = \langle \langle \vec{S} \cdot \hat{n} \rangle \hat{n} \rangle$
 - ↓ Particles near a phase space point
 - Average over phase space

Spin-orbit coupling resonances in circular accelerators

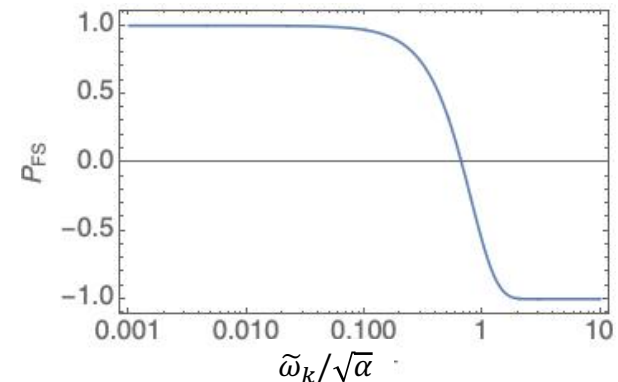
- \hat{n} deviates from \hat{n}_0 near spin-orbit coupling resonances

$$\nu_s = k + k_x \nu_x + k_y \nu_y + k_z \nu_z, \quad k, k_x, k_y, k_z \in \mathbb{Z}. \quad \text{Note that } \nu_s \approx \nu_0 \text{ for small amplitude of orbital motion}$$

- In a planar ring without solenoids, \hat{n}_0 is normally vertical, but could deviate from vertical near integer spin resonances, driven by horizontal magnetic field, for example from misaligned quadrupoles

$$\nu_0 = k, k \in \mathbb{Z}$$

- ✓ In synchrotron/booster, crossing an integer spin resonance could lead to polarization loss, note the Fourier harmonic of integer spin resonances $\tilde{\omega}_k$
- ✓ In an electron storage ring, as will be shown later, the tilt of \hat{n}_0 from vertical direction, associated with $\tilde{\omega}_k$, contribute to the non-resonant spin diffusion of first-order spin resonances



Self-polarization build-up vs radiative depolarization

- Disregard the radiative depolarization, the self-polarization due to Sokolov-Ternov effect would reach P_∞ along \hat{n}_0 , in a time scale of τ_p

$$P_\infty = -\frac{8}{5\sqrt{3}} \frac{\oint \frac{\hat{n}_0 \cdot \hat{b}}{|\rho|^3} d\theta}{\oint \frac{1 - \frac{2}{9}(\hat{n}_0 \cdot \hat{s})^2}{|\rho|^3} d\theta}, \quad \frac{1}{\tau_p [\text{s}]} \approx \frac{2\pi}{99} \frac{E[\text{GeV}]^5}{C[\text{m}] \rho[\text{m}]^2}$$

- The equilibrium beam polarization considering also the radiative depolarization is P_{eq} along the direction $\langle \hat{n}(\vec{z}, \theta) \rangle_{\vec{z}}$, in a time scale of τ_{DK}

$$P_{eq} \approx \frac{P_\infty}{1 + \tau_p / \tau_d}, \quad \frac{1}{\tau_{DK}} = \frac{1}{\tau_p} + \frac{1}{\tau_d}$$

The equilibrium beam polarization has the same amplitude around the ring, independent of phase space location, due to the sufficient phase space mixing given that $\tau_{\text{orb,damp}} \ll \tau_{DK}$

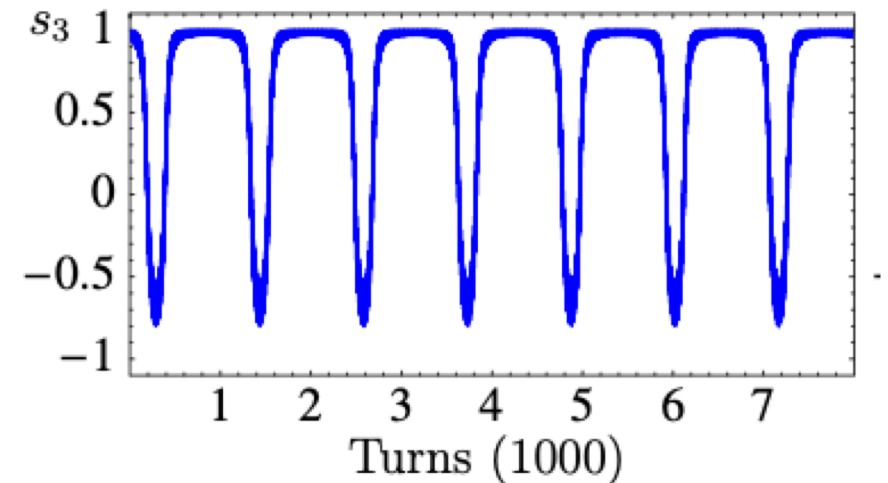
Two views of influence of synchrotron motion on spin motion

The “Static picture” [1]

- The **amplitude-dependent spin tune ν_s** is a function of only orbital actions J_x , J_y and J_z
- $\hat{n}(\vec{z}, \theta)$ is a function of θ and orbital phases (angles).

The “dynamic picture” [2]

- \hat{n} is explicitly time-independent, synchrotron motion is added by hand.
- The **instantaneous spin precession rate ν** is dependent on the instantaneous energy deviation δ ,
$$\nu \approx a\gamma_0(1 + \delta)$$
- Since $\nu_z \ll 1$, **ν looks like a slowly varying ν_0**
- underlying spin resonances could be crossed as a result of synchrotron oscillations, or synchrotron radiation, or the combined effect.



[1] The vertical spin component of one particle during 7 synchrotron periods. While the particle energy oscillates, the reference energy of the ring remained constant.

[1] Hoffstatter, High-energy polarized proton beams, Springer Tracts in Modern Physics, Vol 218, 2006.

[2] Derbenev, Kondratenko and Skrinsky, Part. Accel. 9, 247 (1979)

Theories of radiative depolarization

- Stochastic photon emissions break the adiabatic invariant $J_s = \vec{S} \cdot \hat{n}$
- Much different relaxation time scales of spin and orbit motion

- Non-resonant spin diffusion [1,2,3]
 - Away from main spin resonances

We follow the derivation by Shatunov (2001). Also consult figure 50 for the vectors \mathbf{n} and $\delta\mathbf{n}$ before and after a photon emission. Denote the average spin projection along \mathbf{n} by S_n , and neglect the Sokolov-Ternov terms. Then

$$\delta S_n = (\mathbf{S}_n \cdot \delta\mathbf{n}) = S_n (\mathbf{n} \cdot \delta\mathbf{n}) + S_{\perp} \mathfrak{N}(\mathbf{k}^* \cdot \delta\mathbf{n}). \quad (27.27)$$

Here \mathbf{k} is the generalization of the vector $\mathbf{k}_0 = \mathbf{l}_0 + i\mathbf{m}_0$, i.e. a solution of the spin precession equation and orthogonal to \mathbf{n} . Because the radiation does not depend on the spin phase, the term in S_{\perp} averaged over many photon emissions yields zero. The resulting change to S_n is diffusive: it is of the second order in the fluctuations, i.e.

$$\delta S_n \simeq -\frac{1}{2} (\delta\mathbf{n})^2 S_n, \quad (27.28)$$

which yields

$$\frac{dS_n}{dt} = -\frac{1}{2} S_n \left\langle \left| \gamma \frac{\partial \mathbf{n}}{\partial \gamma} \right|^2 \frac{d(\delta\gamma/\gamma)^2}{dt} \right\rangle_{\theta} \equiv -\alpha_+ S_n, \quad (27.29)$$

Modern notation $\left| \frac{\partial \hat{n}}{\partial \delta} \right|^2$

where recall $\delta\mathbf{n} \simeq -(\hbar\omega_{ph}/E)\gamma (\partial\mathbf{n}/\partial\gamma)$. Equation (27.29) is identical to equation (4.46) in Baier (1972), with appropriate changes of notation. Recall also from (9.9) that

$$\frac{d(\delta\gamma/\gamma)^2}{dt} = \frac{55}{24\sqrt{3}} \frac{e^2 \hbar \gamma^5}{m^2 c^2} \frac{1}{|\rho|^3}. \quad (27.30)$$

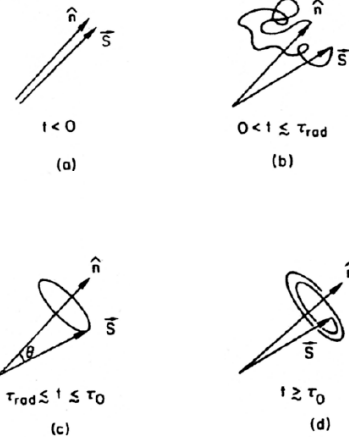
Hence

$$\alpha_+ = \frac{5\sqrt{3}}{8} \frac{e^2 \hbar \gamma^5}{m^2 c^2} \frac{11}{18} \left\langle \frac{d\theta}{|\rho|^3} \left| \gamma \frac{\partial \mathbf{n}}{\partial \gamma} \right|^2 \right\rangle. \quad (27.31)$$

This is the $(11/18)|\gamma (\partial\mathbf{n}/\partial\gamma)|^2$ term in (27.23). This is spin diffusion: the value of the average spin projection S_n evolves diffusively due to terms of second order in the fluctuations (the first-order fluctuations average to zero).

- [1] Derbenev, Kondratenko, Sov. Phys. JETP, 37, 968 (1973)
- [2] Derbenev, Kondratenko and Skrinsky, Part. Accel. 9, 247 (1979)
- [3] Mane et al., Rep. Prog. Phys. 68, 1997, (2005)

- Resonant spin diffusion [4,5,2]
 - Fast, uncorrelated, repetitive crossing of a spin resonance



Chao, AIP Conf Proc 87, 395, 1982

The formula (1) is the starting point in the present paper, and it can be obtained on the basis of simple arguments, which clarify the physical meaning. The quantum fluctuations in the particle momentum during the emission of radiation give rise to a stochastic straying of the detuning $\epsilon_k \equiv \nu - \nu_k$ as a result of the mixing of the particle trajectories in the inhomogeneous field. It then becomes possible for the resonances to be transmitted with velocity $\dot{\epsilon}_k$ equal to

$$|\dot{\epsilon}_k| \sim \langle \epsilon_k^2 \rangle^{1/2} / \tau_r,$$

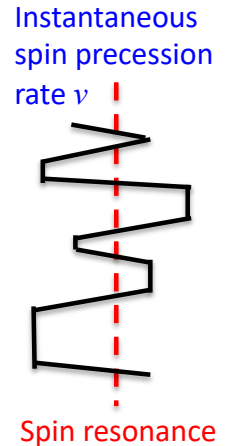
where τ_r is the radiative trajectory-mixing time (τ_r^{-1} is of the order of the decrement of the radiative damping: $\tau_r^{-1} \sim \gamma^3 e^2 m^{-1} |\dot{\mathbf{v}}|$, $\gamma = (1 - v^2)^{-1/2}$ is the relativistic factor, and e , m , and $\dot{\mathbf{v}}$ are the electron charge, mass, and acceleration respectively). Under conditions of rapidity of transmission ($|w_k|^2 \ll |\dot{\epsilon}_k|$), the change in the component of the particle-spin vector \mathbf{s} along the direction \mathbf{n} is equal to [8, 9]

$$\Delta s_n = (s^2 - s_n^2)^{1/2} (2\pi |w_k|^2 / |\dot{\epsilon}_k|)^{1/2} \cos(\Phi_k + \pi/4),$$

where w_k , $\dot{\epsilon}_k$, and Φ_k are the values of the power, the transmission velocity, and the phase of the spin precession at the instant when $\epsilon_k = 0$.

Let $f(I_\alpha)$ be the stationary distribution function of the particles over the action variables I_α of the orbital motion. The number of passages of a resonance per unit time is equal to $|\dot{\epsilon}_k| \int f \delta(\nu - \nu_k) d\Gamma$. Then we obtain for the mean rate $\bar{\xi}$ of change of ξ the expression

$$\bar{\xi} = \bar{s}_n = \int dI_\alpha f(I_\alpha) |\dot{\epsilon}_k| \delta(\nu - \nu_k) \frac{1}{2} \frac{\partial}{\partial s_n} (s_n^2 - s_n^2) = -\pi \langle |w_k|^2 \delta(\nu - \nu_k) \rangle,$$



$$\tau_d^{-1} = \pi \sum_k \langle |w_k|^2 \delta(\nu - \nu_k) \rangle,$$

- [4] Derbenev and Kondratenko, Sov. Phys. Dokl. 19, 438 (1975)
- [5] Kondratenko, Sov. Phys. JETP, 39, 592 (1974)

Non-resonant spin diffusion in a planar ring at high beam energies

$$\hat{n} = \hat{n}_0 \sqrt{1 - |\zeta|^2} + \mathcal{R}(\hat{k}_0^* \zeta) \quad \frac{\partial \hat{n}}{\partial \delta} \approx \mathcal{R} \left(\hat{k}_0^* \frac{\partial \zeta}{\partial \delta} \right) \quad \frac{d\zeta}{d\theta} = -i\vec{\omega} \cdot \hat{k}_0 \sqrt{1 - |\zeta|^2} + i\vec{\omega} \cdot \hat{n}_0 \zeta \quad \vec{\omega} = \vec{\omega}_z \delta + \vec{\omega}_x x_\beta + \vec{\omega}_y y_\beta$$

- First-order “parent” spin resonance
 - $\nu_0 \pm \nu_z = k$ are more important

$$\vec{\omega}_z = \frac{-R[(1 + a\gamma_0)(G_x \eta_x + Q_y \eta_y) - \frac{1}{\rho_x}] \vec{e}_y}{+R[(1 + a\gamma_0)(G_y \eta_y + Q_x \eta_x) - \frac{1}{\rho_y}] \vec{e}_x}$$

$$\frac{\tau_p}{\tau_d} \approx \frac{11}{18} \sum_{k=n-l}^{n+l} \frac{\nu_0^2 |\tilde{\omega}_k|^2 + (\nu_0 - k)^2 |\tilde{\lambda}_k|^2}{[(\nu_0 - k)^2 - \nu_z^2]^2}$$

$$\vec{e}_y \cdot \hat{k}_0 = i \sum_{k=-\infty}^{\infty} \frac{\tilde{\omega}_k e^{i(\nu_0 - k)\theta'}}{\nu_0 - k}$$

$$(1 + a\gamma_0) R G_y \eta_y \vec{e}_x \cdot \hat{k}_0 = \sum_{k=-\infty}^{\infty} \tilde{\lambda}_k e^{i(\nu_0 - k)\theta}$$

Vertical projection of $\vec{\omega}_z$ onto \hat{k}_0 , tilt of \hat{n}_0 from vertical due to integer spin resonances.

Horizontal projection of $\vec{\omega}_z$ onto \hat{k}_0 , due to vertical dispersions [2]

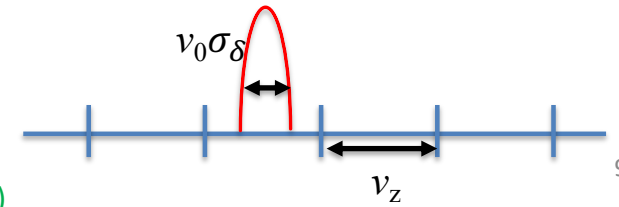
For vanishing ν_z , reduces to [1]

$$\frac{\tau_p}{\tau_d} \approx \frac{11}{18} \sum_{k=n-l}^{n+l} \frac{\nu_0^2 |\tilde{\omega}_k|^2}{(\nu_0 - k)^4}$$

- [1] Derbenev, Kondratenko and Skrinsky, Part. Accel. 9, 247 (1979)
 [2] Montague, Phys. Rep, 113, 1 (1984). [3] Yokoya, Part. Accel. 13, 85 (1983)

- Higher-order synchrotron sideband spin resonances[1,3]
 - $\nu_0 \pm m\nu_z = k$ are more important
 - Modulation index $\sigma = \frac{\sigma_0}{\nu_z} = \frac{\nu_0 \sigma_\delta}{\nu_z}$

$$\frac{\tau_p}{\tau_d} \approx \frac{11}{18} \sum_{k=n-l}^{n+l} \sum_{m=-\infty}^{\infty} \left(\frac{\nu_0^2 |\tilde{\omega}_k|^2 e^{-\sigma^2} I_m(\sigma^2)}{[(\nu_0 - k - m\nu_z)^2 - \nu_z^2]^2} + \frac{(\nu_0 - k)^2 |\tilde{\lambda}_k|^2 e^{-\sigma^2} I_m(\sigma^2)}{[(\nu_0 - k - m\nu_z)^2 - \nu_z^2]^2} \right)$$



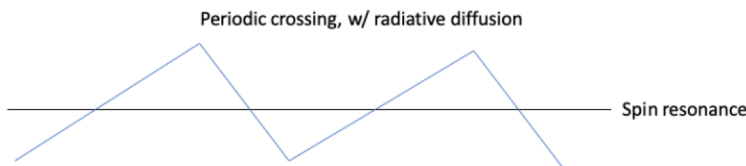
Correlated and uncorrelated regime of spin resonance crossing

- Follow the “dynamical picture” [1] that the **instantaneous spin precession rate ν** is dependent on the instantaneous energy deviation δ , underlying spin resonances could be crossed as a result of synchrotron oscillations
- The following two regimes of spin resonance crossing were also proposed in [1]

- Correlated regime: $\kappa = \frac{\nu_0^2 \lambda_p}{\nu_z^3} \ll 1$

- Non-resonant spin diffusion & perturbative treatment of $\frac{\partial \hat{n}}{\partial \delta}$ applies

$$\frac{\tau_p}{\tau_d} \approx \frac{11}{18} \sum_{k=n-l}^{n+l} \sum_{m=-\infty}^{\infty} \left(\frac{\nu_0^2 |\tilde{\omega}_k|^2 e^{-\sigma^2} I_m(\sigma^2)}{[(\nu_0 - k - m\nu_z)^2 - \nu_z^2]^2} + \frac{(\nu_0 - k)^2 |\tilde{\lambda}_k|^2 e^{-\sigma^2} I_m(\sigma^2)}{[(\nu_0 - k - m\nu_z)^2 - \nu_z^2]^2} \right)$$



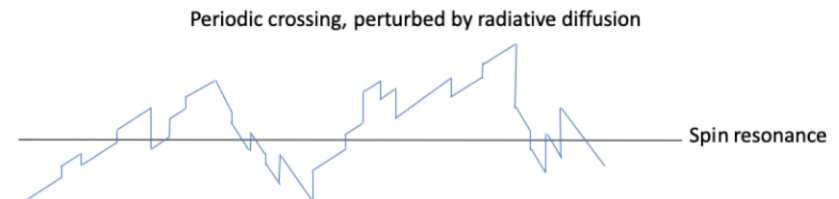
- Uncorrelated regime:

$$\kappa = \frac{\nu_0^2 \lambda_p}{\nu_z^3} \ll 1 \text{ is violated and } \frac{\nu_0 \sigma \delta}{\nu_z} \gg 1$$

- Resonant spin diffusion

$$\lambda_d = \pi \sum_k \langle |\tilde{\epsilon}_k|^2 \delta(\nu - k) \rangle$$

$$\frac{\tau_p}{\tau_d} \approx \frac{\sqrt{\pi/2}}{\lambda_p} \sum_{k=n-l}^{n+l} \frac{|\tilde{\omega}_k|^2}{\sigma_0} \exp\left[-\frac{(\nu_0 - k)^2}{2\sigma_0^2}\right]$$

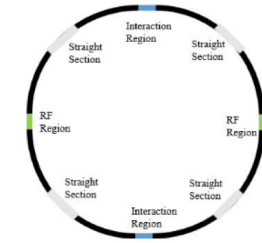


Outline

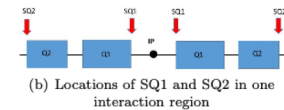
- Radiative depolarization theories
- **Simulation setup**
- Comparison between the theories and simulations

CEPC CDR imperfection lattice seed setup

- Imperfection lattice seed
 - Alignment and field error are introduced, without BPM errors so far
 - Closed orbit & optics correction in SAD & AT.
 - The vertical emittance is adjusted to the design value
 - Quadrupoles in straight sections are artificially rotated
 - Skew quads inserted next to Q1 & Q2
- Translated from SAD to BMAD/PTC for spin tracking



(a) Straight sections of the CEPC



(b) Locations of SQ1 and SQ2 in one interaction region

TABLE I. CEPC magnets' errors.

Component	Misalignment error			Field error
	$\Delta x (\mu\text{m})$	$\Delta y (\mu\text{m})$	$\Delta \theta_z (\mu\text{rad})$	
Dipole	-	-	-	0.01%
Arc quadrupole	100	100	100	0.02%
IR quadrupole	50	50	50	-
Sextupole	100	100	100	-

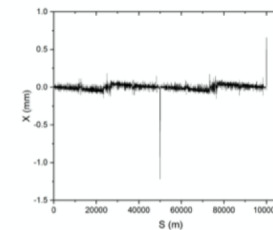
TABLE III. Emittances and fractional tunes of the CEPC at 45.6 GeV calculated by SAD, Bmad and PTC.

	SAD	Bmad	PTC
Horizontal emittance (nm-rad)	0.1731	0.1738	0.1733
Vertical emittance (pm-rad)	1.615	1.623	1.612
Longitudinal emittance ($\mu\text{m-rad}$)	0.9017	0.8956	0.9028
Fractional horizontal tune	0.108	0.108	0.108
Fractional vertical tune	0.217	0.217	0.216
Fractional synchrotron tune	0.028	0.028	0.028

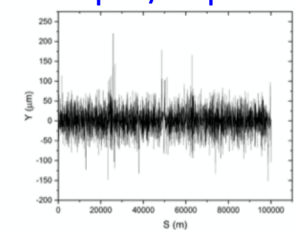
TABLE II. The difference of the closed orbit (CO) and the relative difference of the beta function ($\Delta\beta/\beta$) of the CEPC at 45.6 GeV calculated by SAD, Bmad and PTC. The minus sign indicates the difference between the two codes. "rms" is the root mean square of the difference around the ring. "max" means the maximum absolute value of the difference around the ring.

		$CO_{Bmad-SAD}(\text{m})$	$CO_{PTC-SAD}(\text{m})$	$(\Delta\beta/\beta)_{Bmad-SAD}$	$(\Delta\beta/\beta)_{PTC-SAD}$
Horizontal direction	rms	1.2×10^{-8}	9.5×10^{-8}	6.9×10^{-8}	1.6×10^{-5}
	max	6.8×10^{-8}	3.3×10^{-7}	9.9×10^{-8}	4.2×10^{-4}
Vertical direction	rms	1.4×10^{-10}	1.1×10^{-9}	9.0×10^{-7}	9.5×10^{-5}
	max	1.3×10^{-9}	7.8×10^{-9}	1.4×10^{-6}	6.5×10^{-4}

rms closed orbit are $37\mu\text{m}/28\mu\text{m}$

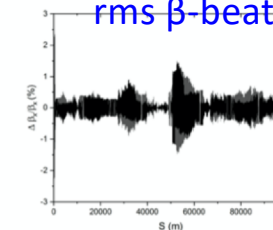


(a) Horizontal closed orbit .

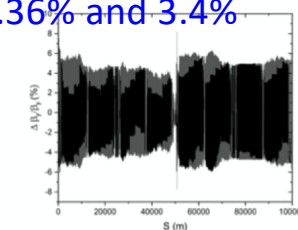


(b) Vertical closed orbit.

rms β -beat are 0.36% and 3.4%



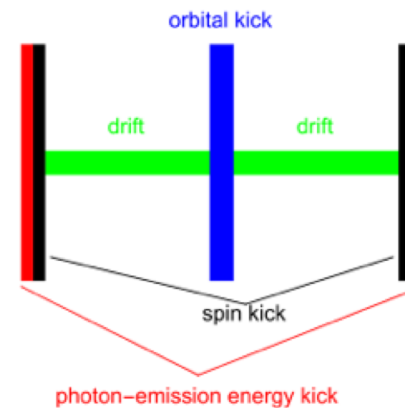
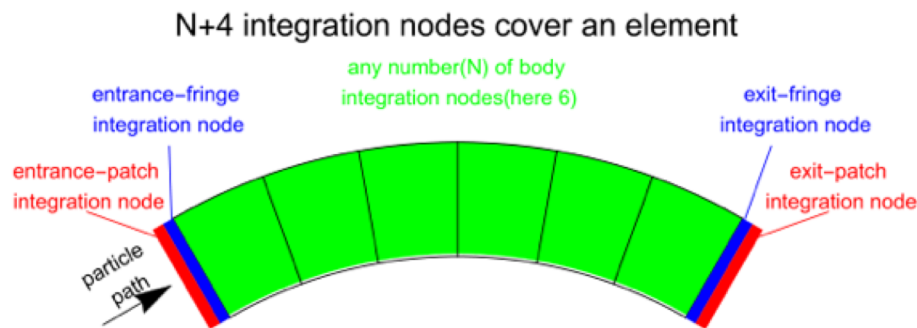
(c) Horizontal beta beating .



(d) Vertical beta beating.

Spin tracking with BMAD/PTC

- In this work, we used the SLIM algorithm of BMAD for simulation of radiative depolarization containing up to first-order spin resonances.
- We then dump the flat file and use PTC to launch Monte-Carlo simulations [1], taking into account of 6D orbital motion and 3D spin motion, as well as realistic synchrotron radiation modeling.
- We are aware of the recent development in BMAD Monte-Carlo simulations and will consider using these advanced features in future studies.



[1] Z. Duan, M. Bai, D. P. Barber and Q. Qin, NIM A793 (2015) 81.

Preparation for analytical estimation of radiative depolarization

- Numerical calculation of harmonics $\tilde{\omega}_k$ and $\tilde{\lambda}_k$

$$\begin{aligned}\tilde{\omega}_k &\approx \frac{1}{2\pi} \int_0^{2\pi R} (1+k)y_0''(s)e^{ik\Phi(s)} ds \\ &\approx \frac{1+k}{2\pi} \sum_{h=1}^M [p_{y,0}(s_{h,2}) - p_{y,0}(s_{h,1})] e^{ik\Phi(s_{h,1})}\end{aligned}$$

$$\begin{aligned}\tilde{\lambda}_k &= \frac{1+k}{2\pi} \int_0^{2\pi R} G_y(s)\eta_y(s)e^{ik\Phi(s)} ds \\ &\approx \frac{1+k}{2\pi} \sum_{h=1}^M G_y(s_{h,1})\Delta s_h \eta_y(s_{h,1}) e^{ik\Phi(s_{h,1})}\end{aligned}$$

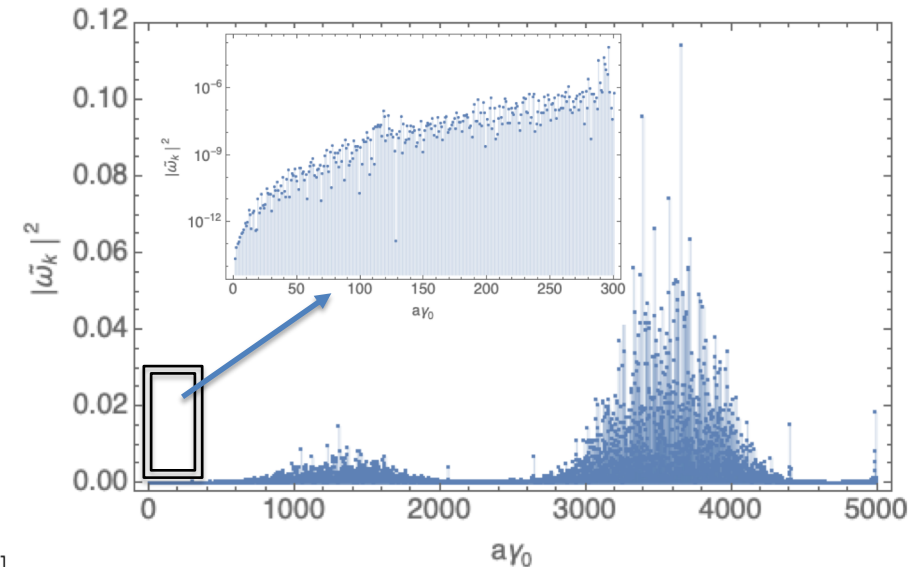
- First-order theory

$$\frac{\tau_p}{\tau_d} \approx \frac{11}{18} \sum_{k=n-l}^{n+l} \frac{\nu_0^2 |\tilde{\omega}_k|^2 + (\nu_0 - k)^2 |\tilde{\lambda}_k|^2}{[(\nu_0 - k)^2 - \nu_z^2]^2}$$

- Correlated & uncorrelated regimes

$$\begin{aligned}\frac{\tau_p}{\tau_d} &\approx \frac{11}{18} \sum_{k=n-l}^{n+l} \sum_{m=-\infty}^{\infty} \left(\frac{\nu_0^2 |\tilde{\omega}_k|^2 e^{-\sigma^2} I_m(\sigma^2)}{[(\nu_0 - k - m\nu_z)^2 - \nu_z^2]^2} \right. \\ &\quad \left. + \frac{(\nu_0 - k)^2 |\tilde{\lambda}_k|^2 e^{-\sigma^2} I_m(\sigma^2)}{[(\nu_0 - k - m\nu_z)^2 - \nu_z^2]^2} \right)\end{aligned}$$

$$\frac{\tau_p}{\tau_d} \approx \frac{\sqrt{\pi/2}}{\lambda_p} \sum_{k=n-l}^{n+l} \frac{|\tilde{\omega}_k|^2}{\sigma_0} \exp\left[-\frac{(\nu_0 - k)^2}{2\sigma_0^2}\right]$$

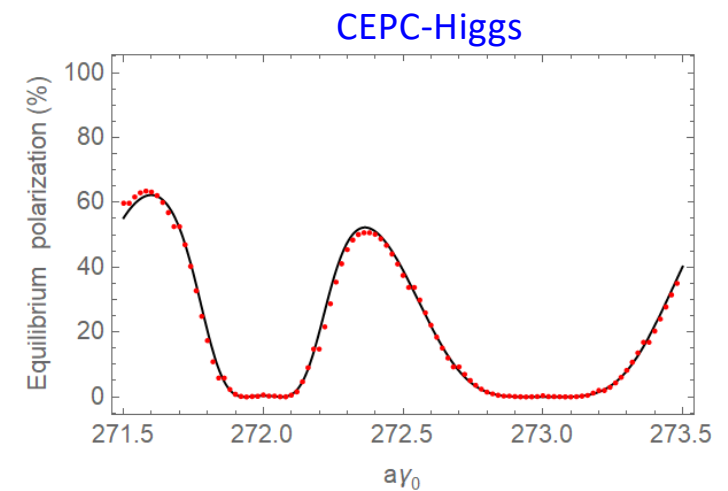
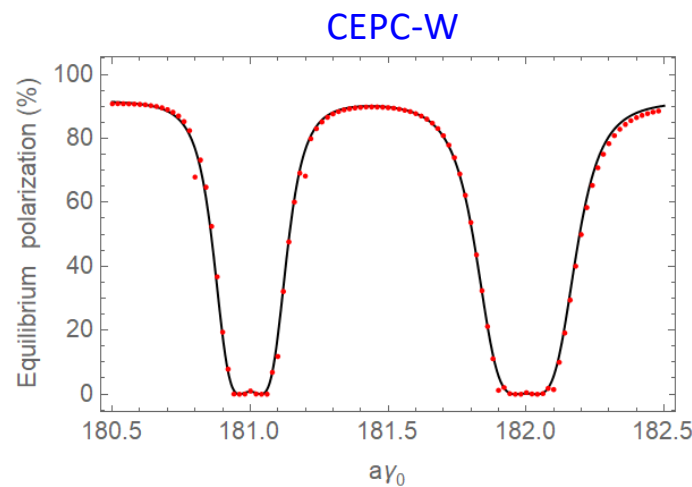
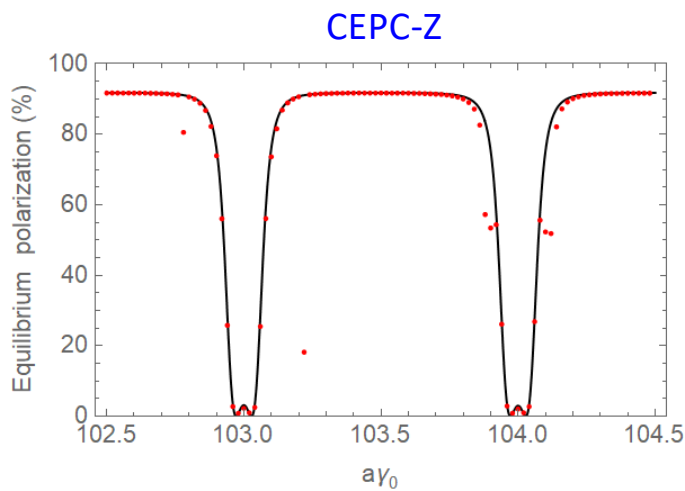
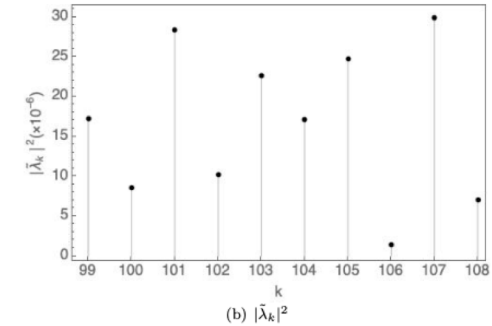
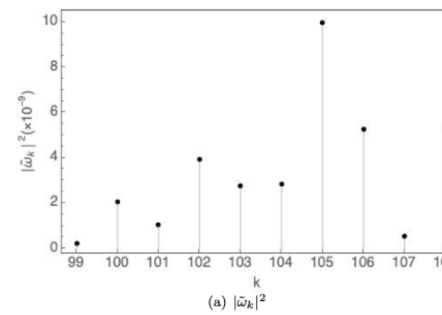


SLIM simulations vs. first-order theory

- First-order theory: $\frac{\partial \hat{n}}{\partial \delta}$ with only contributions from first-order “parent” spin resonances $\nu_0 \pm \nu_z = k$

$$\frac{\tau_p}{\tau_d} \approx \frac{11}{18} \sum_{k=n-l}^{n+l} \frac{\nu_0^2 |\tilde{\omega}_k|^2 + (\nu_0 - k)^2 |\tilde{\lambda}_k|^2}{[(\nu_0 - k)^2 - \nu_z^2]^2}$$

- Retain only the two nearest harmonics in the evaluation



Outline

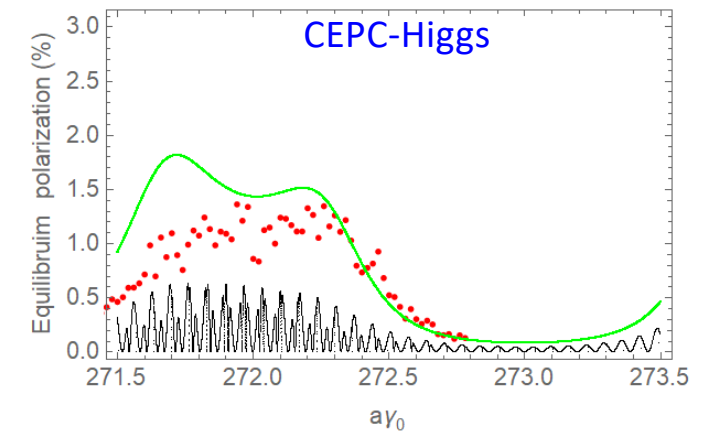
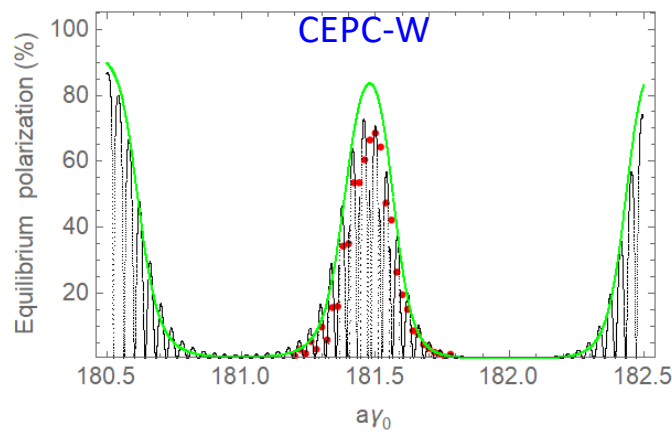
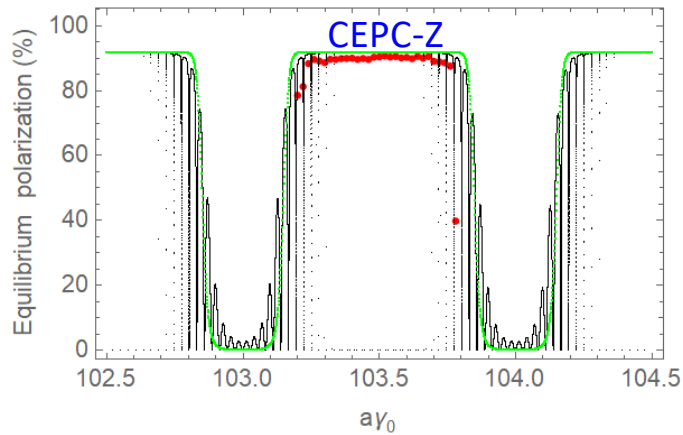
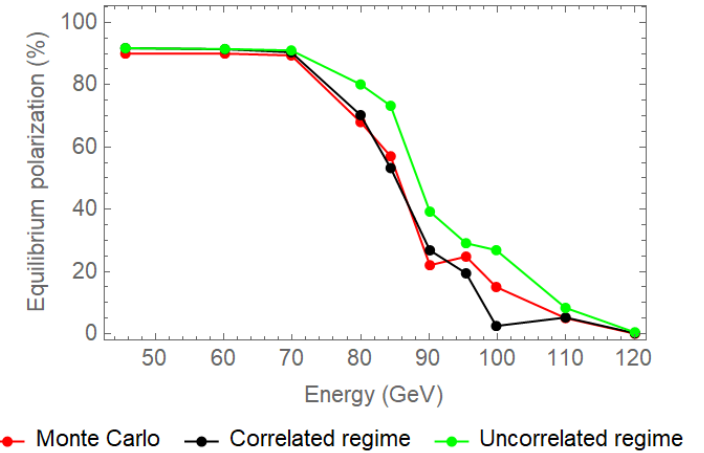
- Radiative depolarization theories
- Simulation setup
- Comparison between the theories and simulations

Case study: dependence on beam energy

- Increasing beam energy lead to larger σ_δ , modulation index σ and correlation index κ

TABLE IV. The CEPC lattice parameters. (* indicates the planned operation energies in the CEPC CDR.)

Beam energy (GeV)	$a\gamma_0$	$ \tilde{\omega}_k ^2 (\times 10^{-9})$	$ \tilde{\lambda}_k ^2 (\times 10^{-5})$	$\sigma_\delta (\times 10^{-4})$	ν_z	τ_p (h)	κ	σ
45.6*	103.5	$ \tilde{\omega}_{103} ^2 = 2.7$ $ \tilde{\omega}_{104} ^2 = 2.8$	$ \tilde{\lambda}_{103} ^2 = 2.2645$ $ \tilde{\lambda}_{104} ^2 = 1.7166$	3.77	0.028	252.72	0.03	1.39
60.1	136.5	$ \tilde{\omega}_{136} ^2 = 3.7$ $ \tilde{\omega}_{137} ^2 = 14.7$	$ \tilde{\lambda}_{136} ^2 = 0.8178$ $ \tilde{\lambda}_{137} ^2 = 5.5717$	4.96	0.028	63.34	0.20	2.42
69.8	158.5	$ \tilde{\omega}_{158} ^2 = 6.6$ $ \tilde{\omega}_{159} ^2 = 26.4$	$ \tilde{\lambda}_{158} ^2 = 0.9574$ $ \tilde{\lambda}_{159} ^2 = 4.4585$	5.77	0.0324	30.00	0.36	2.82
80.0*	181.5	$ \tilde{\omega}_{181} ^2 = 14.4$ $ \tilde{\omega}_{182} ^2 = 53.3$	$ \tilde{\lambda}_{181} ^2 = 4.9118$ $ \tilde{\lambda}_{182} ^2 = 15.6433$	6.61	0.0395	15.24	0.52	3.04
84.4	191.5	$ \tilde{\omega}_{191} ^2 = 16.3$ $ \tilde{\omega}_{192} ^2 = 19.8$	$ \tilde{\lambda}_{191} ^2 = 15.5332$ $ \tilde{\lambda}_{192} ^2 = 1.0088$	6.97	0.0425	11.65	0.61	3.14
90.1	204.5	$ \tilde{\omega}_{204} ^2 = 19.1$ $ \tilde{\omega}_{205} ^2 = 43.8$	$ \tilde{\lambda}_{204} ^2 = 3.7786$ $ \tilde{\lambda}_{205} ^2 = 0.6403$	7.43	0.0467	8.39	0.72	3.25
95.4	216.5	$ \tilde{\omega}_{216} ^2 = 15.0$ $ \tilde{\omega}_{217} ^2 = 34.8$	$ \tilde{\lambda}_{216} ^2 = 6.1547$ $ \tilde{\lambda}_{217} ^2 = 1.2292$	7.88	0.0515	6.31	0.80	3.31
99.8	226.5	$ \tilde{\omega}_{226} ^2 = 10.5$ $ \tilde{\omega}_{227} ^2 = 27.4$	$ \tilde{\lambda}_{226} ^2 = 35.2604$ $ \tilde{\lambda}_{227} ^2 = 4.9787$	8.24	0.0550	5.03	0.90	3.39
109.9	249.5	$ \tilde{\omega}_{249} ^2 = 56.9$ $ \tilde{\omega}_{250} ^2 = 41.3$	$ \tilde{\lambda}_{249} ^2 = 26.9851$ $ \tilde{\lambda}_{250} ^2 = 46.9963$	9.08	0.0585	3.10	1.48	3.87
120.1*	272.5	$ \tilde{\omega}_{271} ^2 = 770.4$ $ \tilde{\omega}_{272} ^2 = 95.8$ $ \tilde{\omega}_{273} ^2 = 1684.2$	$ \tilde{\lambda}_{271} ^2 = 41.6290$ $ \tilde{\lambda}_{272} ^2 = 12.0825$ $ \tilde{\lambda}_{273} ^2 = 361.7036$	9.90	0.0650	2.03	1.95	4.15



• Monte Carlo • Correlated regime • Uncorrelated regime

• Monte Carlo • Correlated regime • Uncorrelated regime

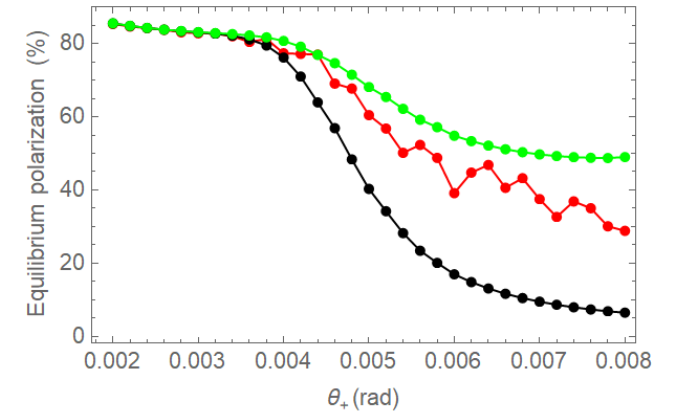
• Monte Carlo • Correlated regime • Uncorrelated regime

Case study: dependence on wiggler parameters at Z-pole

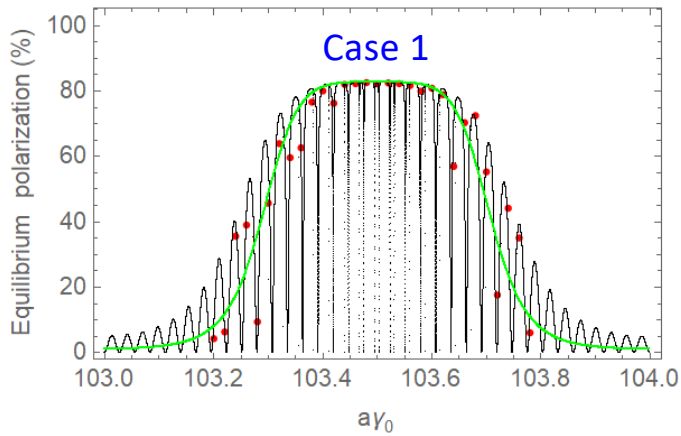
- Asymmetric wigglers are employed to boost self-polarization build-up at Z-pole.
- The influence of various wiggler settings are simulated and compared to theories.

TABLE V. Beam parameters for various wiggler settings

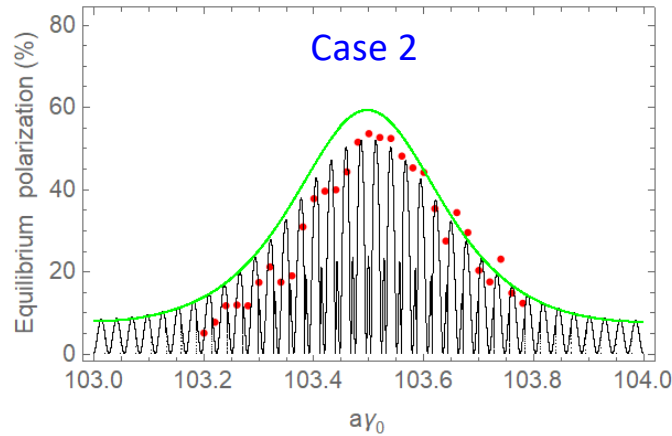
wigglers	θ_+ (rad)	U_0 (MeV)	$\sigma_\delta (\times 10^{-4})$	τ_p (h)	κ	σ
w/o	-	36.1	3.77	252.8	0.03	1.39
Case 1	0.0033	43.9	9.53	32.3	0.22	3.52
Case 2	0.0056	60.0	17.26	7.2	1.00	6.38
Case 3	0.0080	84.8	24.55	2.5	2.85	9.07



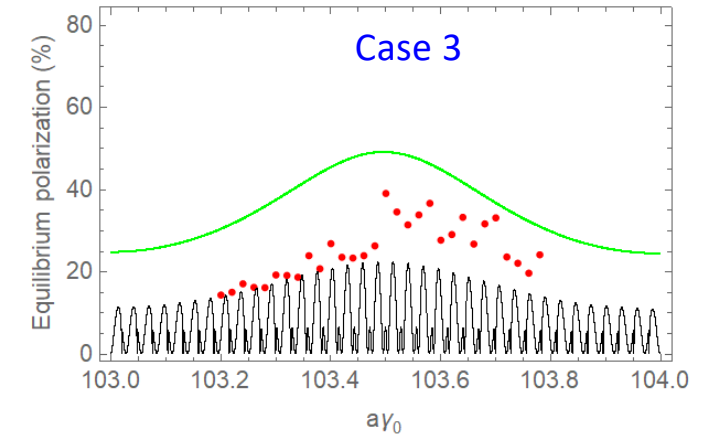
—●— Monte Carlo —●— Correlated regime —●— Uncorrelated regime



—●— Monte Carlo —●— Correlated regime —●— Uncorrelated regime



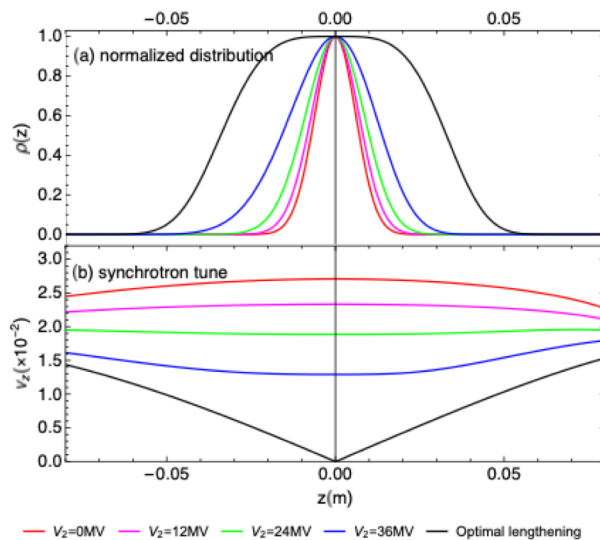
—●— Monte Carlo —●— Correlated regime —●— Uncorrelated regime



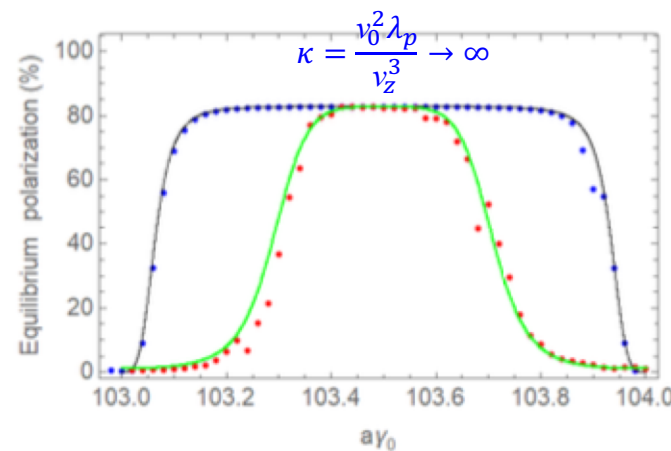
—●— Monte Carlo —●— Correlated regime —●— Uncorrelated regime

Case study: influence of harmonic RF cavity at Z-pole

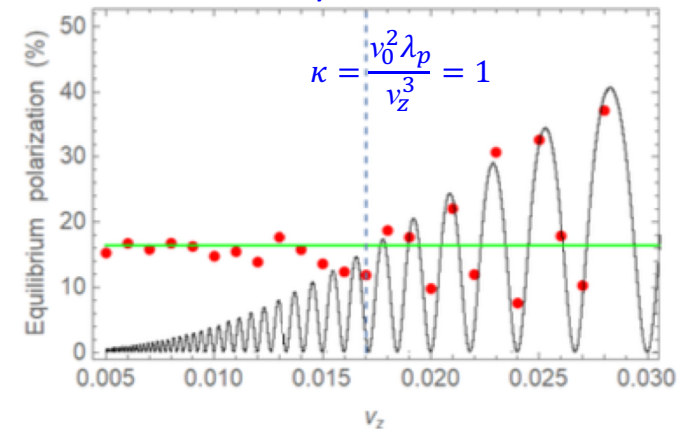
- A double-RF system was proposed as a viable mitigation to the X-Z instability due to beam-beam[1].
- The synchrotron tune ν_z and its distribution among beam particles affects both the modulation index σ and the correlation index κ . Various double-RF settings are simulated.
- Findings:
 - The optimal lengthening case with vanishing ν_z at zero amplitude, agrees with “uncorrelated regime”
 - There seems to be a transition from the correlated regime to uncorrelated regime, with decreasing ν_z at zero amplitude.



optimal lengthening condition



Scan the voltage of the passive harmonic system



• SLIM • First-order theory • Monte Carlo • Uncorrelated regime • Monte Carlo • Correlated regime • Uncorrelated regime

[1] M. Migliorati et al., EPJP 136, 1190 (2021).

Summary

- We compared Monte-Carlo simulation of the radiative depolarization versus the two distinct theories that describe the influence of synchrotron oscillations & radiations at ultra-high beam energies.
- The comparison suggests a gradual evolution from the correlated regime to the uncorrelated regime, not clear at the moment. Work urgent is needed to clarify the theory. For example using the Bloch equation[1,2,3], that could merges into these theories at extremes.
- Generation of this study to more comprehensive lattice modeling and more error seeds is foreseen, for better understanding the radiative depolarization mechanisms and establishing correction methods to achieve a high beam polarization @ CEPC.

Thank you for your attention!